Acoustic Analysis of Composite Soft Materials III: Compressibility of Boundary Layers around Particles of Mica and Calcium Carbonate

Masahiro Maebayashi, Shinya Otsuka, Tatsuro Matsuoka, Shinobu Koda

Department of Molecular Design and Engineering, Graduate School of Engineering, Nagoya University, Chikusa-ku, Nagoya 464-8603, Japan

Received 8 November 2004; accepted 18 March 2005
DOI 10.1002/app.22304
Published online in Wiley InterScience (www.interscience.wiley.com).

ABSTRACT: The velocities of longitudinal, transverse, and leaky surface skimming compressional waves (LSSCW) of polyvinylchloride composite materials were measured as a function of the particle concentration. The mica and calcium carbonate (CC) particles were used as additives. The longitudinal and transverse velocities for the PVC/mica composite increased with the concentration of the mica. In the case of the PVC/CC composite, the transverse velocity increased with the concentration of the CC particle, but the longitudinal velocity was independent of the concentration. The LSSCW velocity for the polyvinylchloride matrix did not change in each composite. The partial specific volume and the partial specific adiabatic compressibility of each particle dispersed in polyvinylchloride were evaluated from sound velocity and density data. The compressibility of the boundary layer around the particles was estimated. The thickness of the boundary layer around the mica particle was estimated. For the PVC/CC composite, on the other hand, a softer phase than the PVC matrix was formed around the CC particle because the compressibility of the boundary layer was larger than that of the PVC matrix.
 J Appl Polym Sci 98: 1385–1392, 2005

Key words: composites; interface; partial specific compressibility; polyvinylchloride (PVC); sound velocity

INTRODUCTION

To elucidate the effect of dispersed fillers on polymer composite materials, it is necessary to evaluate not only the bulk mechanical and elastic properties of the materials but also those properties of the matrix region and local parts, such as the boundary layer. In many cases, the mechanical and elastic properties of polymer composite materials have been evaluated by several methods, such as the impact test, dynamic mechanical analysis, and differential scanning calorimetry, and molecular properties are investigated by some spectroscopies.[1–6]

The interface or the boundary layer between the filler and the matrix has been sometimes investigated through the observation of the fracture surface by using a scanning electron microscope (SEM) or an atomic force microscope (AFM). Fu and coworkers indicated that the cavity around the filler in the composite consisting of the high density polyethylene matrix and the calcium carbonate particles is influenced by the particle size and the distance between the particles.[7] Lazzeri and colleagues introduced that the thickness of the immobilized layer of polymer around the fillers can be obtained from volume strain measurements.[8] They reported that the thickness of the immobilized layer of polypropylene adhering to calcium carbonate particles is fairly thin. The SEM and AFM are used to investigate the morphology of the fracture surface. However, it is difficult to determine the mechanical or elastic properties near the interface quantitatively.

The acoustic analysis for composite materials gives not only the elastic property of the entire sample but also information about the local region in composite materials, such as the matrix and boundary layer.[9–13] Moreover, acoustic methods are nondestructive methods because the elastic properties of the specimen are evaluated from the velocity and absorption of the elastic wave propagating in the specimen. The scanning acoustic microscope (SAM) has been used predominantly for the evaluation of the elastic property in metallic materials.[14–16] A few examples of applications to polymer materials are also reported.[17] In these works, the SAM is operated in the frequency range 10 to 500 MHz, where the wavelength of the acoustic

Correspondence to: S. Koda (koda@nuce.nagoya-u.ac.jp).
Sponsor: Japan Society for the Promotion of Science, Grant-in-Aid for Scientific Research on Priority Areas (A); contract grant number: 13031044, 2001 and 14045235, 2002.
Contract grant sponsor: 21st century COE program "Nature Guided Materials Processing" of the Ministry of Education, Culture, Sports, Science and Technology.

wave in water is between 3 and 150 μm at 25°C. The lateral resolution of the acoustic micrograph obtained by the SAM is slightly less than the wavelength for water, which is used as a coupling fluid between the acoustic lends and the specimen. If the diameter of the particles dispersed in composites is larger than the wavelength, the system is considered to be inhomogeneous acoustically.[18] We have investigated previously the morphology and sound velocity of plasticized PVC by the SAM.[19] The three structures defined by Liu and colleagues were observed in our acoustic micrographs of PVC composites.[20–22] The LSSCW velocity of the matrix region decreases with structural changes from the well-dispersed structure to the flocculated structure.

The frequency range of the acoustic waves used in the pulse method is generally between 1 and 10 MHz, and then the wavelength of the acoustic waves is between 0.2 and 3 mm for polymeric materials. The wavelength of the acoustic waves is usually larger than the particle size in the composite, and the composite is regarded as an acoustically homogeneous system in this frequency range. Therefore, the particles have no direct effect on the detected acoustic signal. The change in the elastic properties, which stems from addition of the particles, leads to that in the velocity of the acoustic waves. We investigated the boundary layer around the spherical particle in the systems of PVC-PMMA-BR and PVC/glass composites.[10,23] The compressibility of the boundary layer around the BR was comparable to that of BR particles, and that around the glass particles was more rigid than that of the PVC matrix and the thickness of the layer was a few micrometers. The shapes of the BR and the glass particles used in the previous study were almost the sphere. The model developed in our previous study can be applied to any composites that involve particles of an undefined shape.

In this work, we tried to apply the three states model to the composite, including the nonspherical particles, and to evaluate the elastic property of the boundary layers around the particles in the PVC composite materials from density and acoustic wave velocity measurements and analysis of the acoustic micrograph on the basis of the three states model. The morphology of the PVC composite material and the velocity of LSSCW of the PVC matrix were investigated by the SAM. The pulse method using the time to amplitude converter was applied to obtain the velocity of bulk longitudinal and transverse waves propagating in the PVC composite materials.

EXPERIMENTAL

Sample preparation

PVC powders were kindly supplied by Kaneka Chemical Co. Ltd. The average size of the PVC grain particle was about 150 μm. The molecular weight of the PVC was approximately 40,000. The mica particle (PDM-7–80) was supplied by TOPY Industries Ltd. The nominal particle size (φ) distribution of the mica was as follows; $\varphi > 300$ μm: less than 5 wt %, 300 μm $> \varphi >$100 μm: 35–60 wt %, $\varphi <$ 100 μm: 30–60 wt %. The calcium carbonate (CC) particles of the average size 11 and 27 μm were supplied by Shiraishi Kogyo Ltd., and those of the average particle size 100 and 300 μm were supplied by Ohtori Seiko Ltd. Methyl tin isooctyl tioglycolate supplied by Kohsei Co., Ltd. was used as a stabilizer of the PVC matrix to prevent release of the HCl gas by heat in the molding process of the samples.

PVC samples with different particle concentrations were prepared by the following procedure. PVC powders and each particle were mixed with the stabilizer at 50 rpm for an hour. The molding temperatures were set to produce a transparent part in the center of the specimen molded. The molding temperature for the PVC/mica composites was 160°C, and that of the PVC/CC composites was 180°C. The mixed raw products were maintained at 160 or 180°C under the pressure of 3.0 MPa by using a hot press and a ring of stainless for 15 min. They were cooled down to the ambient temperature at the rate of 12°C $\cdot$ min^{-1} after the molding. The volume content of the stabilizer added in all the samples was 0.95%. A plasticized sample disc of 100 mm diameter and 2 mm thickness was obtained. The PVC disk used in this study consisted of three regions, which were responsible for the distribution of the stress and temperature within the disc. The center of the disc was transparent, and the edge was white because the agglomerate of the PVC was not dissolved completely. In this work, the center (well-dispersed structure) part was used for the density and velocity measurements.

Velocity measurements

Bulk acoustic wave velocities at the frequency of 5 MHz were obtained by measuring the time required for transmission through a specimen of thickness (l). To determine a transmission time precisely, the pulse method with the time-to-amplitude converter (TAC) was used in a double transducer system. Lead zirconate titanate (PZT) and *X*-cut quartz were used to generate the transverse and longitudinal waves, respectively. Details of this experimental method are described in the literature.[24] The frequency of 5 MHz was chosen so that the scattering of the acoustic wave by an immersed particle did not influence theoretically the velocity measurements.[25]

The velocity (V) was calculated from the following equation:

$$V = l/t \tag{1}$$

where t is the transmission time through the specimen. The l is the thickness of the specimen. The l was the averaged value for five points on the specimen measured by using a micrometer. The velocity measurements were carried out at 25.0 ± 0.1°C. The experimental error of the velocity measurements in this work was within ± 10 m • s^{-1}.

The longitudinal modulus (M), the shear modulus (G), and the bulk modulus (K) were calculated from the following equations, respectively.

$$M = dV_l^2 \tag{2}$$

$$G = dV_t^2 \tag{3}$$

$$K = M - (4/3)G \tag{4}$$

where V_l and V_t are the longitudinal and transverse wave velocities, respectively, and d is the density of the specimen. Poisson's ratio (σ) was calculated by the following equation in the case of isotropic materials:

$$\sigma = [(3K - 2G)/2(3K + G)]. \tag{5}$$

The adiabatic compressibility (κ) is the reciprocal of the bulk modulus K.

$$\kappa = K^{-1}. \tag{6}$$

The velocity of the LSSCW propagating on the surface of the specimen was measured by a reflection-type scanning acoustic microscope (HSAM-210, Hitachi Kenki Fine Teck Co., Ltd. and RTX-1, Honda Electronics Co., Ltd.). A $V(z)$ curve was measured by varying the distance (z) between the sample and the acoustic lens. The velocity of LSSCW can be calculated from the following equation[14,18]:

$$V_{lsscw} = V_w/[1 - (1 - V_w/2f\Delta z)^2]^{1/2} \tag{7}$$

where V_w is the longitudinal wave velocity in water and f is the frequency of the acoustic wave. Δz is the defocus distance between successive minima in the $V(z)$ curve. In the velocity measurement, a frequency of 100 MHz was used, and the velocity was measured by using water as a coupling fluid. The temperature of the specimen was measured by a thermocouple placed on the sample surface and was controlled at 25.0 ± 0.1°C. The experimental error of the LSSCW velocity measurements was within ± 20 m • s^{-1}.

Observation of acoustic micrographs

All acoustic micrographs were observed by employing the point focus lens (Honda Electronics Co., Ltd.: UPF-4A). The semiaperture angle and the focal length of the lens were 60° and 0.5 mm, respectively. The frequency of the acoustic wave was 400 MHz, and the theoretical lateral resolution on the sample surface immersed in water was about 4 μm.[18] The focal plane of the acoustic wave was set to the sample surface so that the amplitude of the reflected wave from the PVC matrix was the greatest amplitude. The difference in the intensity of the reflected wave from the sample surface gives the contrast of the acoustic micrograph.

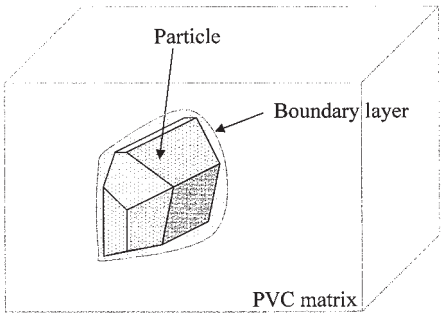

Figure 1 Schematic diagram of three states model. The model consists of the particle, polymer matrix, and boundary layer between the particle and the matrix.

When the acoustic wave enters into the sample with incident angle of 0°, the reflection coefficient at the sample-water interface denoted by R is determined from the following equation:

$$R = \frac{|Z_l - Z_w|}{Z_l + Z_w} \tag{8}$$

where Z_l and Z_w are acoustic impedances of the longitudinal waves propagating in the sample and water as the coupling fluid, respectively. The acoustic impedance is the product of the density and the velocity ($Z = dV$) in each medium. The acoustic impedance is expressed as the elasticity divided by the velocity of the acoustic wave. The large reflected signal is detected when the acoustic impedances of the specimen are different largely from water.

Density measurements

Density measurements were carried out by a water immersion method by using a pycnometer at the temperature of 25.0 ± 0.1°C. The fine air bubble was eliminated from the cut surface of the specimen by degassing in the vacuum desiccator. The experimental error was within ± 2 kg • m^{-3}

ANALYSIS OF EXPERIMENTAL DATA

We reported earlier that the three states model, as shown in Figure 1, could be applied to polymer composites in which particles were dispersed.[10,23]

The volume of a composite is given by the following equation when the volume additivity between the PVC matrix and that in the boundary layer holds[26,27]:

$$V = (n_m - n_b n_p)v_m + n_p(v_p + n_b v_b) \quad (9)$$

where v_m, v_p, and v_b are the specific volumes of the PVC matrix, the particle, and the boundary layer, respectively. The n_m and n_p are the mass of the matrix polymer and the dispersed particle, and n_b is the mass ratio of the polymer in the boundary layer to which the particle is added. The partial specific volume of the dispersed particle is obtained as the derivative of eq. (9) by n_p:

$$\bar{v}_p = v_p + n_b(v_b - v_m). \quad (10)$$

The limiting partial specific compressibility for the dispersion particle is defined by:

$$\bar{\kappa}_p^0 = -\frac{1}{\bar{v}_p^0}\left(\frac{\partial \bar{v}_p}{\partial p}\right)_{S,0}. \quad (11)$$

The subscript zero refers to the value where the concentration of dispersion particles approaches zero. The terms S and p denote the entropy and the pressure of the system, respectively. From eqs. (10) and (11), the following equation is derived:

$$\bar{\kappa}_p^0 = \frac{v_p}{\bar{v}_p^0}\kappa_p + \frac{n_b}{\bar{v}_p^0}(v_b\kappa_b - v_m\kappa_m) \quad (12)$$

where κ_p, κ_b, and κ_m are the compressibility of the particle, the boundary layer, and the matrix, respectively. If it is assumed that the partial specific volume of the particle is equal to the specific volume of that, the first term represents the compressibility of the particle itself. The second term contains information about the boundary layer and the matrix.

The partial specific volume and the partial adiabatic compressibility of the particle are obtained experimentally from the following equations[26]:

$$\bar{v}_p^0 = \lim_{x\to 0}\left(1 - \frac{d-x}{d_m}\right)\frac{1}{x} \quad (13)$$

$$\bar{\kappa}_p^0 = -\frac{\kappa_m}{\bar{v}_p^0}\lim_{x\to 0}\left(\frac{d-x}{d_m} - \frac{\kappa}{\kappa_m}\right)\frac{1}{x} \quad (14)$$

where x is the concentration of the dispersed particles (kg • m^{-3}). d_m and d are densities of the matrix and entire specimens, respectively. κ is the adiabatic compressibility of the composite material at the particle concentration, which is indicated by x, respectively.

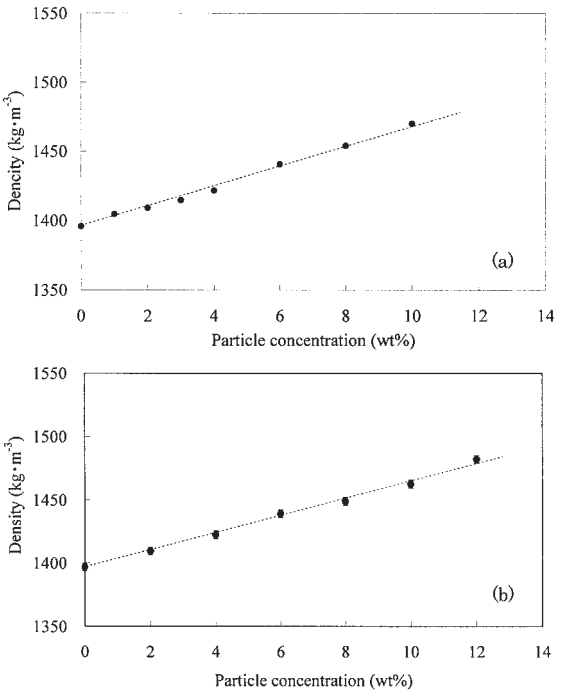

Figure 2 Concentration dependence of the density measured on (a) PVC/mica and (b) PVC/CC composites.

EXPERIMENTAL RESULTS

Figure 2 shows the concentration dependence of the density of the PVC/mica and PVC/CC composites. The densities increase linearly with the increase of the particle concentration for each composite. As particle size dependence is not observed in the case of the PVC/CC composite, the densities are averaged at each concentration of the CC particle. The increment of the density for the PVC/CC composite is smaller than that of the PVC/mica composites.

The concentration dependences of the longitudinal wave velocity for the PVC/mica and PVC/CC composites are shown in Figure 3. As the longitudinal velocities of the PVC/CC composites were almost constant even if the CC particle size changed, the velocity shown in Figure 3b and used in the analysis is averaged at each concentration. The velocity of the PVC/CC composite is constant in the concentration range from 0 to 12 wt % within experimental error. The velocity of the PVC/mica composite linearly increases with the concentration of the mica particle. The velocity of the mica free PVC sample in Table I is slightly faster than that of the CC free PVC sample. The difference is caused by the molding temperature. As we mentioned in the Experimental section, the molding temperature of the PVC/mica composite was set to 160°C, but that of the PVC/CC composite was 180°C. Faunker indicated through SEM images that the collapse of the PVC grain particle is affected by the molding temperature.[28]

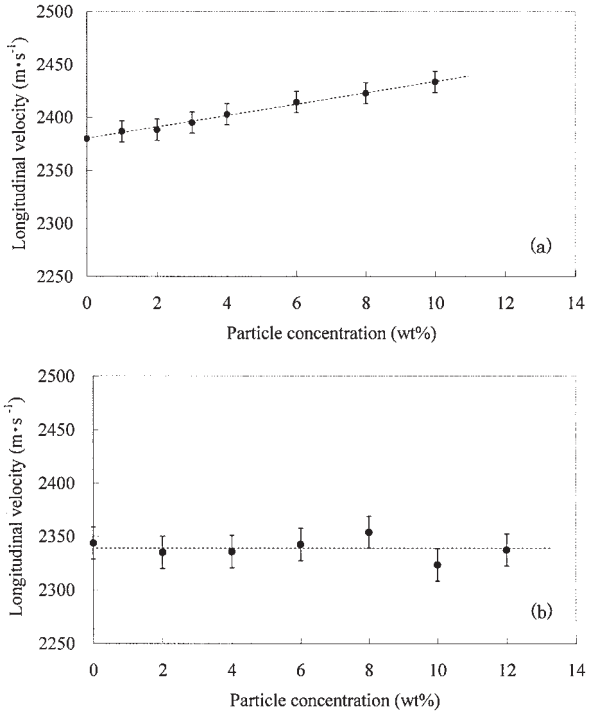

Figure 3 Concentration dependence of the longitudinal wave velocity for (a) PVC/mica and (b) PVC/CC composites.

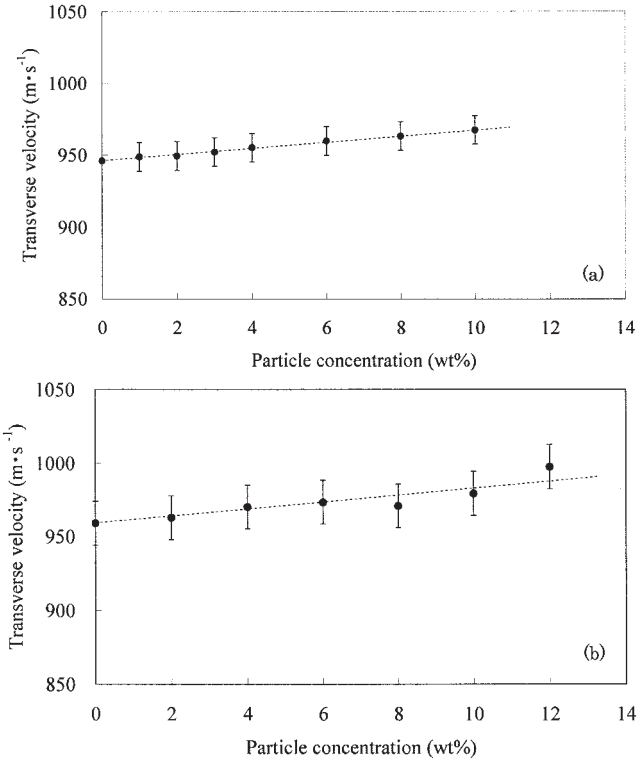

Figure 4 Concentration dependence of velocity of the transverse wave for (a) PVC/mica and (b) PVC/CC composites.

Figure 4 shows the plots of the transverse wave velocity against the particle concentration for the PVC/mica and PVC/CC composites. The increment of the transverse velocity against that of the particle concentration is smaller than that of the longitudinal velocity. Although the longitudinal velocity of the PVC/CC composite doesn't change with the increase of the CC particle, the transverse velocity increases with the concentration of the particle.

The particle concentration dependence of Poisson's ratio of each composite obtained from the density and the velocity data is shown in Figure 5. Poisson's ratio is also equal to 0.405 ± 0.003 in all the PVC/mica composites, and the value is nearly equal to Poisson's ratio of PVC/glass composites.[23] Poisson's ratio of the PVC/CC composite decreases with the concentration of the CC particle.

TABLE I
Density and Longitudinal Velocity of the Specimen without Particles

Particle type	d_0 / kg · m^{-3}	$V_{1,0}$ / m · s^{-1}
Mica	1396	2380
Calcium carbonate	1397	2351
Glass*	1396	2389

* referred from the result of a previous study.[22]

Figure 6 shows acoustic micrographs of the surface of PVC composites in which mica and CC particles are dispersed. Although a good contrast cannot be obtained by the optical micrograph because the optical refractive index of the particle is almost the same as that of PVC, a definitive contrast is obtained in the acoustic micrograph because of the large difference in the acoustic impedances between the particles and the PVC matrix. Since the contrast of the acoustic micrograph reflects the difference in the elastic modulus, bright parts in Figure 6 correspond to the particle having larger modulus than the PVC matrix. Some parts darker than the matrix part observed in Figure 6 are traces of the unstuck particles. The prominent bright rings around the particle due to the interference between the reflected waves from the sample surface and from the PVC-glass interface are observed in the case of the PVC/glass composite.[23] However, the rings are not observed in Figure 6 because the irregular surface of the mica and CC particles disturbs the phase of the reflected wave from the PVC-particle interface. The particle immersed in the matrix cannot be observed in the micrograph when the distance between the particle and the surface of the PVC composites is longer than the penetration depth of the acoustic wave. The penetration depth determined in the case of the PVC matrix is less than 20 μm in the frequency of 400 MHz.

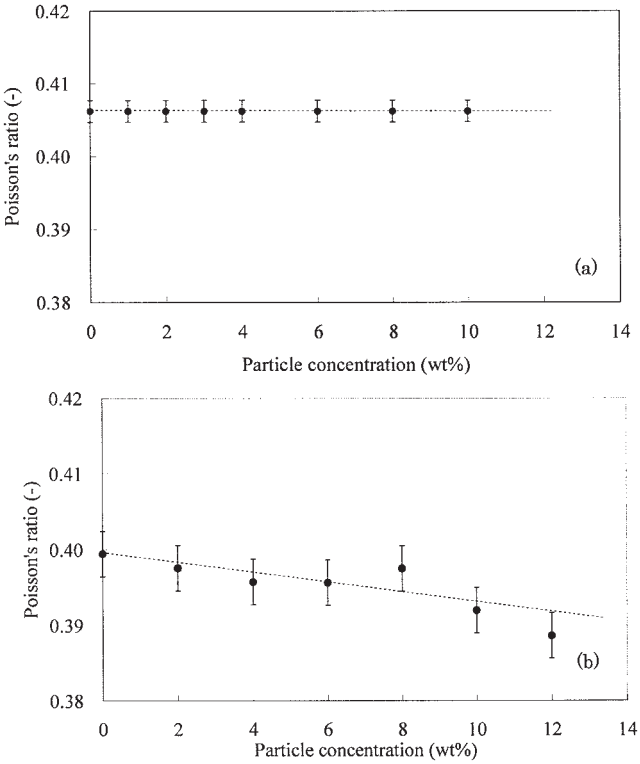

Figure 5 Concentration dependence of the Poisson's ratio of (a) PVC/mica and (b) PVC/CC composites obtained from velocity and density data.

For specimens containing CC particles whose average particle size is 300 μm, the velocities of the LSSCW in the PVC matrix parts in which the particles do not exist near the surface are shown in Figure 7. The value of the LSSCW is the averaged one measured in several points in the composite. It is well known that the velocity of LSSCW is nearly equal to that of the bulk longitudinal wave propagating in polymer materials.[18] The velocities are almost constant and are independent of the particle sizes and concentrations. The PVC matrix is considered to be homogeneous acoustically. There is a slight difference between the velocities of the bulk longitudinal wave for PVC itself and the LSSCW for PVC matrix parts without particles. In a previous article, similar results were obtained for PVC/glass composites.[23] The LSSCW velocity for PVC composites including the mica or small CC particles whose concentration was more than 3 wt % was not measured because the normal $V(z)$ curve was not obtained due to the fine particles found in the measuring area. The LSSCW velocity of the PVC/CC composite molded at the temperature of 180°C is also slower than the velocity of the PVC/glass composite molded at the temperature of 160°C.[23]

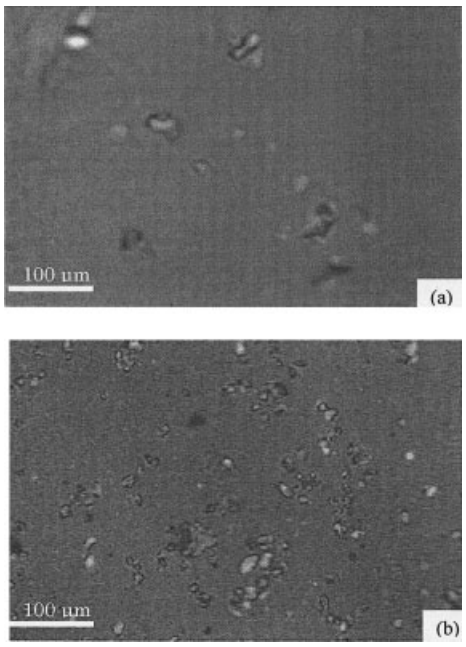

Figure 6 Acoustic micrographs of the PVC composites in which the (a) micas and (b) CC particles are dispersed. The frequency of the acoustic wave is 400 MHz.

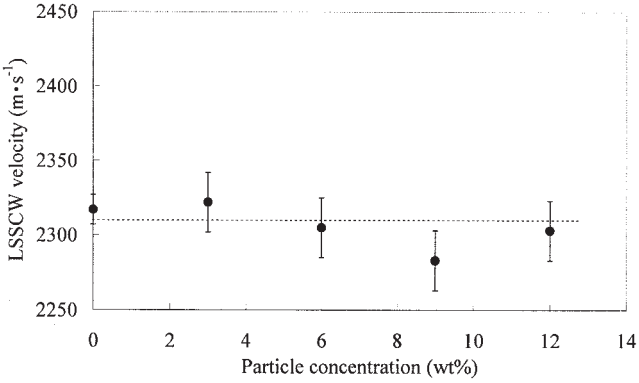

Figure 7 Concentration dependence of the LSSCW velocities measured on the PVC matrix part of the PVC/CC composite. The particle size of the CC particle is 300 μm.

The plots of $(d\text{-}x)/d_m$ and the compressibility ratio (κ/κ_m) against the concentration of mica and CC particles are given in Figure 8. The values of $(d\text{-}x)/d_m$ and the compressibility ratio are almost linearly proportional to the particle concentration, respectively. The values of $(d\text{-}x)/d_m$ and the compressibility ratio in the concentration range less than 100 kg · m^{-3} are used in the estimation of the partial specific volume and the partial specific adiabatic compressibility. One can estimate the specific volume and compressibility from the slopes in Figure 8 by using eqs. (13) and (14). These results for each particle are summarized in Table II. The partial specific volumes are equal to specific volumes of each particle.

DISCUSSION

The three states mode is applicable to analysis of polymeric composite materials when a polymer ma-

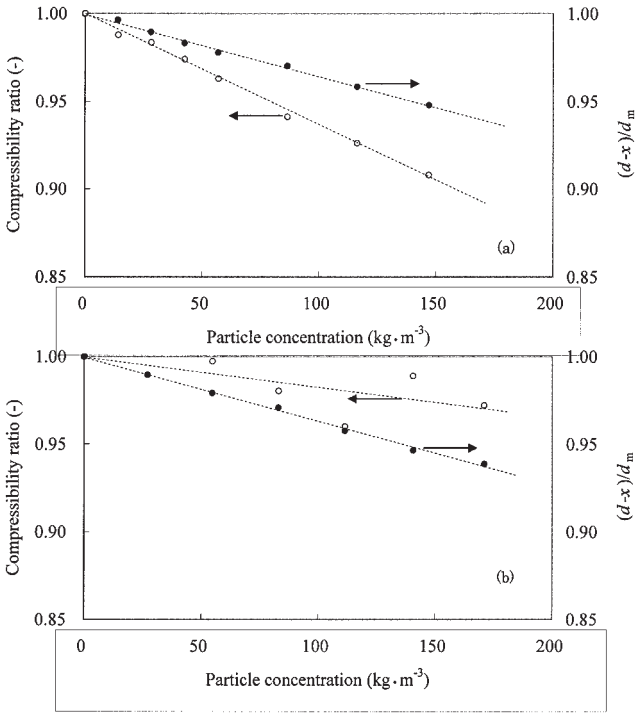

Figure 8 Plots of $[1 - (d\text{-}x)/d_m]$ and compressibility ratio against the particle concentration (x) for (a) PVC/mica and (b) PVC/CC composites.

trix is homogeneous.[10] As described in the Results section, the PVC matrix in PVC composites investigated here is regarded as homogeneous acoustically. From Table II, the specific volumes of each particle are equal to the partial specific volume, that is, $\bar{v}_p^0 - v_p$. In addition, if the specific volume of the boundary layer is assumed to be equal to that of the PVC matrix, eq. (12) is rewritten as follows:

$$\bar{\kappa}_p^0 = \kappa_p + \frac{n_b v_m}{\bar{v}_p^0}(\kappa_b - \kappa_m). \quad (15)$$

Only two unknown parameters relating to the boundary layer remain in eq. (15). From acoustic micrographs, the thickness of the boundary layer around the particles may be less than the lateral resolution of the acoustic micrograph of 4 μm.

The compressibility of the boundary layer around the mica particle is equal to that around the glass particle, $(0.7 \pm 0.3) \times 10^{-10}$ Pa^{-1},[23] since the chemical composition of mica is similar to that of glass, and the effect of the interaction between the mica and the PVC is considered to be almost the same as that between the glass and the PVC. The mass ratio for the boundary layer around the mica particle thus estimated is in the range from 0.3 to 0.4 kg · kg^{-1}. When the volume of a spherical particle is the same as that of a rectangular particle whose aspect ratio is 10, the surface area of the rectangular particle is about six times larger than that of the spherical particle. The larger mass ratio of the PVC/mica composite is caused by the larger surface area of the mica particle discussed above. In the case of scare-like rectangular particles of which the length of the long axis is 100 μm and the aspect ratio is 10, the thickness of the boundary layer obtained from the mass ratio may be in the range from 3.2 to 3.8 μm. These values are larger than the thickness of the interface region in polymer mixtures or diblock copolymers, which range from 20 to 100 nm.[29,30] The larger values obtained in this work are because the acoustic method gives information about the region where the elastic property of the boundary layer is different from that of the matrix.

In the case of the PVC/CC composite, although the shapes of the CC particles are rectangular solid, triangular pyramid, and so on, it is assumed that all the CC particles are cube to facilitate analysis. When the thickness of the boundary layer is less than 4 μm, which is the lateral resolution of the acoustic micrograph, the upper limits of the mass ratio for the boundary layer around the CC particles obtained through the above assumption is 0.13 kg · kg^{-1}. The compressibility of the boundary layer is larger than 4×10^{-10} Pa^{-1}, which is larger than that of the PVC matrix (1.67×10^{-10} Pa^{-1}). As is shown in Table II, the difference $\bar{\kappa}_p^0 - \kappa_p$ is positive. From eq. (15), this means that the compressibility of the boundary layer (κ_b) is larger than the matrix region (κ_m). At any rate, the boundary layer is softer than the PVC matrix.

Lazzeri and coworkers and Thio and colleagues indicated that the fine CC particles aggregate in the polymer matrix and small amount of air entrapped in

TABLE II
Specific Volume and Compressibility for Mica, Calcium Carbonate, and Glass Particles, and Partial Specific Volume and Partial Specific Adiabatic Compressibility for PVC Composites Involving the Particles

Particle type	v_p / 10^{-3} m^3 · kg^{-1}	κ_p / 10^{-10} Pa^{-1}	$\bar{v}_p^0$ / 10^{-3} m^3 · kg^{-1}	$\bar{\kappa}_p^0$ / 10^{-10} Pa^{-1}
Mica	0.36	0.23	0.36	-1.1 ± 0.5
Calcium carbonate	0.37	0.13	0.37	0.8 ± 0.7
Glass*	0.40	0.25	0.40	0.0 ± 0.5

* referred from the result of a previous study.[22]

the aggregate.[8,31] If air exists in the aggregate, voids are formed in the specimen by expansion when the specimen is heated in the molding. Considering the compressibility of the CC particle and its partial specific volume, we suggest that the PVC/CC composite has a small amount of the fairly soft phase. However, that phase is not observed in some micrographs obtained by optical and acoustic microscopes due to low resolution. The decrease of tensile strength and the increase of Young's modulus with the addition of CC particles have been reported by Wu and coworkers and Zhu and colleagues in the mechanical testing of PVC/nano-CC and PVC/CC composites.[32,33] Wu and coworkers suggested that the decrease of tensile strength with the CC content originated from the poor interaction between the CC particle and the PVC matrix. The soft phase presented in our discussion may be equivalent to the poor interaction layer.

CONCLUSIONS

The elastic property or the thickness of the boundary layer around the particle, which is an undefined shape, is estimated quantitatively by using acoustic techniques and the three states model.

The elastic property of the PVC matrix is not influenced by the addition of particles, since the LSSCW velocity is independent of the concentration of the CC particles. The effect of the addition of particles on the partial specific volume of the particles is not recognized in the case of the PVC/mica and PVC/CC composites. The percentage by mass of the boundary layer around the mica particle against the particle determined on the basis of the three states model is about 40 wt %. The PVC/CC composite has a small amount of the soft phase from the viewpoint of partial specific adiabatic compressibility.

The authors would like to express their appreciation to Kaneka Co. Ltd., Shiraishi Kogyo Ltd., Ohtori Seiko Ltd., TOPY Industries Ltd., and Kohsei Co., Ltd. for providing the basic ingredients of the composites.

References

1. Byrne, C.; Wang, Z. Carbon 2001, 39, 1789.
2. Bomal, Y.; Godard, P. Polym Eng Sci 1996, 36, 237.
3. Tjong, S. C.; Xu, S. A. Polym Int 1997, 44, 95.
4. Fras, I.; Boudeulle. M.; Cassagnau P.; Michel A. Polymer 1998, 39, 4773.
5. Gong, F.; Feng, M.; Zhao, C.; Zhang, S.; Yang, M. Polym Degrad Stab 2004, 84, 289.
6. D-Gutiérrez, S.; R-Pérez, M. A.; Saja, J. A. D.; Velasco, J. I. Polymer 1999, 40, 5345.
7. Fu, Q.; Wang, G.; Shen, J. J Appl Polym Sci 1993, 49, 673.
8. Lazzeri, A.; Thio, Y. S.; Cohen, R. E. J Appl Polym Sci 2004, 91, 925.
9. Chen, J.-Y.; Hoa, S. V.; Jen, C.-K; Viens, M.; Monchalin, J.-P. Polym Compos 1998, 19, 225.
10. Koda, S.; Tsutsuno, N.; Yamada, G.; Nomura, H. J Appl Polym Sci 2089, 2001, 81.
11. Youssef, M. H.; Nasr, G. M.; Gomaa, A. S. Polym Test 2000, 19, 311.
12. Dandekar, D. P.; Boteler, J. M.; Beaulieu, P. A Compos Sci Technol 1997, 58, 1397.
13. Verdier, C.; Piau, M. J Phys D 1996, 29, 1454.
14. Kushibiki, J.; Chubachi N. IEEE Trans Sonics Ultrason 1985, 32, 189.
15. Comte, C.; Stebut, J. Surf Coat Technol 2002, 154, 42.
16. Hirose, N.; Asami, J.; Sato, H.; Yamanaka K. Jpn J Appl Phys 1997, 36, 3260.
17. Duquesne, J. Y.; Yamanaka, K.; Neron, C.; Jen, C. K.; Piche, L.; Lessard, G. Mater Res Soc Symp Proc 1989, 142, 253.
18. Briggs, A. Acoustic Microscopy; Clarendon Press: Oxford, 1992.
19. Yamada, G.; Koda, S.; Matsuoka, T.; Nomura, H. Jpn J Appl Phys 2001, 40, 3593.
20. Liu, Z. H.; Kwak, K. W.; Li, R. K. Y.; Choi, C. L. Polymer 2002, 43, 2501.
21. Liu, Z. H; Zhu, X. G.; Li, Z.; Qi, Z. N.; Wang, F. S. Polymer 1998, 39, 1863.
22. Liu, Z. H.; Zhang, X. D.; Zhu, X. G.; Qi, Z. N.; Wang, F. S; Li, R. K. Y.; Choy, C. L. Polymer 1998, 39, 5027.
23. Maebayashi, M.; Otsuka, S.; Matsuoka, T.; Koda, S. Jpn J Appl Phys 2001, 40, 2939.
24. Koda, S.; Yamashita, K.; Matsumoto, K.; Nomura, H. Jpn J Appl Phys 1993, 32, 2234.
25. Javanaud, C.; Gladwell, N. R.; Gouldby, S. J.; Hibberd, D. J.; Thomas, A.; Robins, M. M. Ultrasonics 1991, 29, 331.
26. Nomura, H.; Miyahara, Y. J Appl Polym Sci 1964, 8, 1643.
27. Nomura, H.; Kawaizumi, F.; Iida, T. Bull Chem Soc Jpn 1987, 60, 25.
28. Faukner, P. G. J Macromol Sci Phys B 1975, 11, 251.
29. Shull, K. R.; Mayes, A. M.; Russell T. P. Macromolecules 1993, 26, 3929.
30. Chaturvedi, U. K.; Steiner, U.; Zak, O.; Krausch, G.; Klein, J. Phys Rev Lett 1989, 63, 616.
31. Thio, Y. S.; Argon, A. S.; Cohen, R. E.; Weinberg, M. Polymer 2002, 43, 3661.
32. Wu, D.; Wnag, X.; Song Y.; Jin, R. J Appl Polym Sci 2004, 92, 2714.
33. Zhu, S.; Zhang, Y.; Zhang, Y.; Zhang, C. Polym Test 2003, 22, 539.